

Third harmonic generation in optical microfibres

Laboratoire interdisciplinaire Carnot de Bourgogne, UMR 5209
CNRS-Université de Bourgogne, 21078 DIJON Cedex, FRANCE

Aurélien Coillet, Philippe Grelu

2012

Using optical microfibers, phase matching between different propagation modes allows for third-harmonic generation (THG). After detailing the relevant phase matching conditions and overlap integrals, we provide a comparison between THG effective efficiencies in silica and tellurite glasses. We also explain the relatively easy, wideband, conversion that we observe experimentally in silica glass microfibers, from 1.55 μm to the green, by the geometry of the tapering region.

1 Introduction

Optical microfibres have attracted a lot of attention over the past few years, owing to their unique optical properties that result from a large field confinement combined with an accessible evanescent field. These properties have permitted the demonstration of various applications, such as miniature lasers [1], sensors [2, 3] and optical trapping [4]. The high step-index contrast of the waveguide, whose diameter is typically sub-wavelength, provides indeed a tight confinement of the electromagnetic field. Thus, compared to the conventional single mode fibres featuring a low step-index contrast, the effective nonlinearity can be enhanced by several orders of magnitude. In addition, the dispersive properties of the microfibre are strongly diameter-dependent. These features justify the interest on microfibres for frequency conversion applications, provided that significant nonlinear effects can take place on propagation lengths as short as a few millimeters. Indeed, an optical microfibre taper is typically drawn with a short length of the order of a few centimeters, a convenient size for experiments where the microfibre is either standing in air or deposited onto a substrate [5]. A series of experiments exploited such increased nonlinearity, accessible in a compact setting, by obtaining supercontinuum generation in silica [6] and chalcogenides microfibres [7]. In recent years, there has been a sustained interest in demonstrating the generation of third-harmonic waves through nonlinear propagation in silica microfibres [8–11].

The use of optical fibres specially designed for third-harmonic generation experiments is also under investigation [12, 13]. Third-harmonic generation (THG) is made possible by a phase-matched third-order nonlinear process between different propagation modes. In the present work, we present our latest results on this topic. We first illustrate the THG process in microfibres by reporting our observations of THG using a silica microfibre taper pumped at around $1.55\ \mu\text{m}$. Then, we detail the relevant phase matching conditions and overlap integrals. We highlight the trade-off between the conversion bandwidth and efficiency, which results from the shape of the tapering region. To provide an outlook with the use of highly-nonlinear non-silica glasses [9, 14], we compare numerically the effective efficiencies of THG in silica and in tellurite microfibres, after taking into account the radiative losses that are calculated using the theory of nonadiabatic intermode transitions [15]. As tellurites and chalcogenides offer large transparency windows extending to the mid-infrared, the possibility of down-converting a pump with three-photon generation in the mid-infrared is considered as an additional perspective.

2 Experimental results in silica

Experimentally, THG can be obtained through a simple setup composed of a pulsed laser source delivering a high peak power of the order of 1 kW, which is directly coupled via a standard FC/APC connector to a tapered silica fibre. In our experiments, microfibres were drawn manually from a standard telecom (SMF-28) fibre, applying the flame-brushing technique down to sub-micron diameters [16]. Despite the absence of automation, overall losses below 1 dB for a 5 cm long taper were routinely achieved. We used a laser source of our making, which was described in Ref. [9]. It produces a train of 400 ps pulses at a 100 kHz repetition rate. Its output peak power can reach 1.5 kW while the average power is kept below 60 mW. The output wavelength can be tuned in the 1550-1560 nm range, with a narrow linewidth smaller than 0.1 nm. Sending these pulses to the microfibre taper, we could detect a third-harmonic beam at around 520 nm, exiting the SMF-28 fibre past the tapering region where it was generated. The presence of scattering on the taper made also the generated green light visible to the naked eye. We recorded its optical spectrum: since only a narrow spectral line was observed at the third-harmonic of the pump, there was no doubt on the origin of the generated light. Thanks to the tunability of the pump source, we found that the same microfibre taper could produce a THG wave for all accessible pump wavelengths, between 1550 to 1560 nm, with approximately the same efficiency, the obtained converted wavelengths ranging from 516 nm to 520 nm. This relatively large conversion bandwidth is a-priori not expected in the case of a phase-matched process. We shall explain such observation in the following section. A typical spectrum is shown on figure 1. Interestingly, we also notice a small amount of signal detected at the second harmonic of the pump wave. Second-harmonic generation, usually not possible in bulk glasses, is attributed to surface interactions [8].

Experimentally, we obtained an average green power of 15 nW with a pumping power

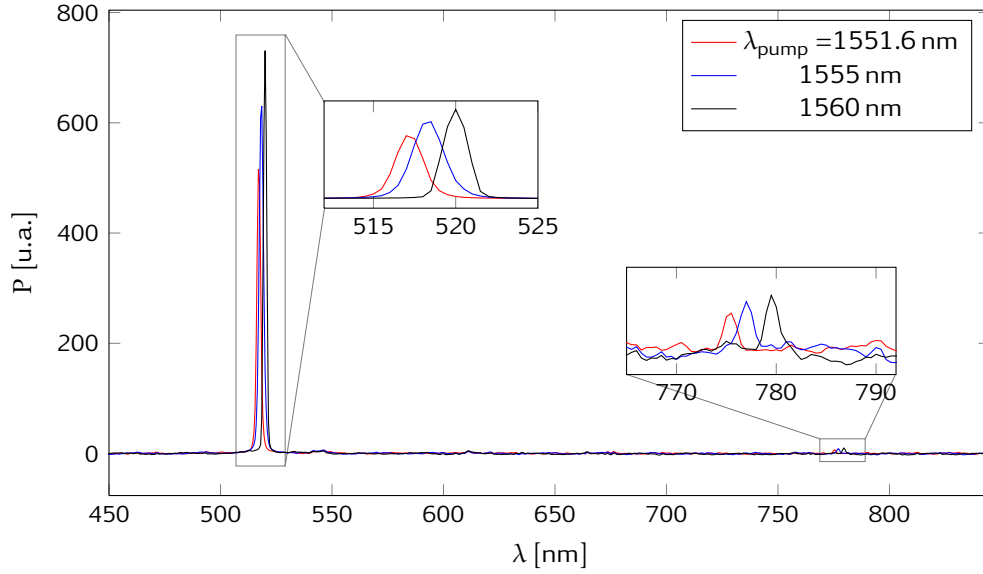


Figure 1: Spectrum of the third-harmonic wave, generated around 520 nm by pumping the same microfibre at three different wavelengths. A small amount of second-harmonic wave around 780 nm is also visible, see its magnification.

of 60 mW, yielding an overall conversion efficiency of 2.5×10^{-7} (2×10^{-9} for the second harmonic). THG is based on $\chi^{(3)}$ interactions and the converted power is expected to increase as P_p^3 , where P_p is the pump power. Indeed, the experimental results reproduce this cubic-law feature, as displayed on Fig.2. Figure 2 also shows the comparable efficiencies obtained at two different pump wavelengths.

3 Phase-matching and overlap integral

According to Grubsky and Feinberg, the THG process in silica microfibres can become efficient when the pump, which is coupled to the fundamental guided mode, is phase-matched to higher-order modes for the third-harmonic wave [17]. In the quasi-continuous regime, by assuming a small amount of generated third-harmonic wave - the undepleted pump approximation-, the evolution of the converted power P_3 along the propagation axis z is calculated to be:

$$P_3(z) = P_p^3 \left(\frac{2\omega n_2 |J_3|}{\delta\tilde{\beta}c} \right)^2 \sin^2 \left(\frac{\delta\tilde{\beta}z}{2} \right), \quad (1)$$

where ω is the pump frequency, n_2 , the nonlinear refractive index of the glass, c , the speed of the light in vacuum, and $\delta\tilde{\beta}$ is the propagation phase constant mismatch between the two modes. The latter is expressed by:

$$\delta\tilde{\beta} = \beta_3 - 3\beta_p + 3\frac{\omega}{c}n_2(2J_2 - J_1)P_p. \quad (2)$$

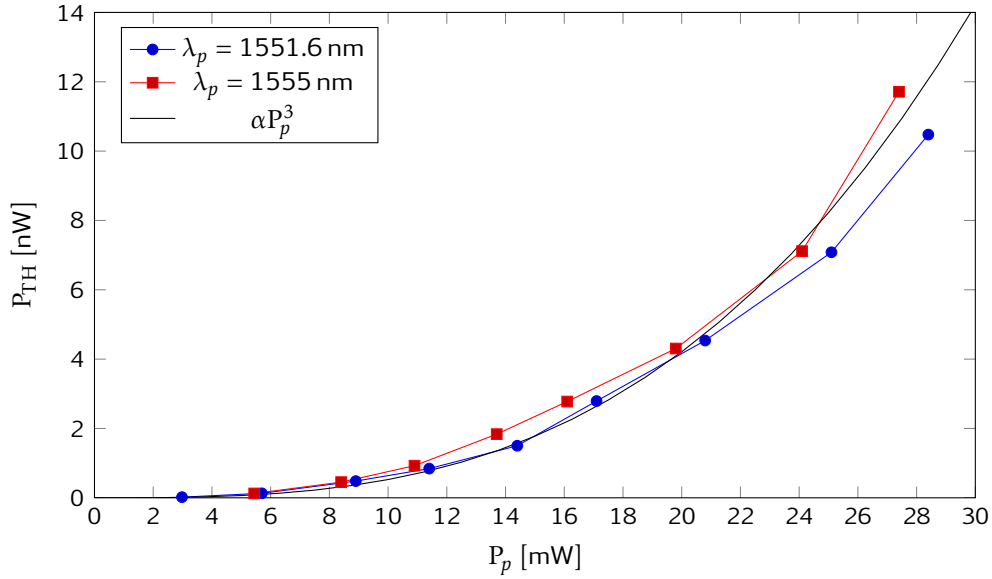


Figure 2: Evolution of the converted THG power as a function of the pump power for two different pump wavelengths. A cubic curve is also plotted for comparison. All powers are measured after propagation in the microfibre.

The last term is a correction for the pump-induced nonlinear phase shift, weighted by the overlap integrals J_1 and J_2 . Since this term only adds a marginal correction to the phase mismatch in the kW-peak power regime of interest here, we left it out in our study. To obtain an efficient conversion, the two important parameters that need to be optimized in Eqn.(1) are the J_3 overlap integral, which should be maximal, and the phase mismatch, which should be minimal. Let us focus on the overlap integral J_3 , which will determine which modes should be efficiently used:

$$J_3 = \int_{A_{nl}} (\mathbf{F}_p^* \cdot \mathbf{F}_3)(\mathbf{F}_p \cdot \mathbf{F}_p^*) dS, \quad (3)$$

where \mathbf{F} stands for the electrical field distribution. The J_3 integral has been calculated for an interaction between the HE_{11} mode of the pump at $\lambda = 1550$ nm and some of the first higher-order modes of the third harmonic (see table 1). TE and TM modes do not overlap with the HE_{11} , as well as even-order modes (such as EH_{21} and HE_{41}). The best overlap integral is obviously obtained between two HE_{11} modes - one at the pump wavelength, and the other one at the third harmonic, but due to the material dispersion, phase-matching cannot be achieved in this situation. Fortunately, several other modes yield J_3 values of the same order of magnitude: EH_{11} , HE_{31} and, especially, HE_{12} . Increasing the order of the mode further decreases the overlap, and we shall therefore focus on the three modes above to find the phase-matching condition.

Assuming that the nonlinear corrections to the phase mismatch are negligible, the phase-matching condition $\delta\tilde{\beta} = 0$ implies the equality of the effective indices of the

Mode	HE ₁₁	EH ₁₁	HE ₃₁	HE ₁₂	EH ₂₁	HE ₄₁	HE ₂₂
$ J_3 [\mu\text{m}^{-2}]$	2	0.863	0.25	1	1.5×10^{-16}	3.3×10^{-17}	4.6×10^{-17}

Table 1: Overlap integral J_3 between the HE₁₁ mode at $\lambda = 1.55\mu\text{m}$ and the first 7 modes at the third-harmonic wavelength. While the overlap integrals are non zero for odd higher-order modes, the values are lower than those presented here.

interacting modes. Figure 3 displays the variations of the effective indices of the modes as functions of the diameter of the silica microfibre, when the wavelength of the pump is set to 1550 nm. We can see that there are particular values of the microfibre diameter where a phase matching condition is fulfilled: for the third-harmonic modes EH₁₁, HE₃₁ and HE₁₂, the phase-matching diameters are $d_p = 625$ nm, 717 nm and 766 nm, respectively. Microfibres with such diameters can be drawn with low losses, hence explaining the observed generation.

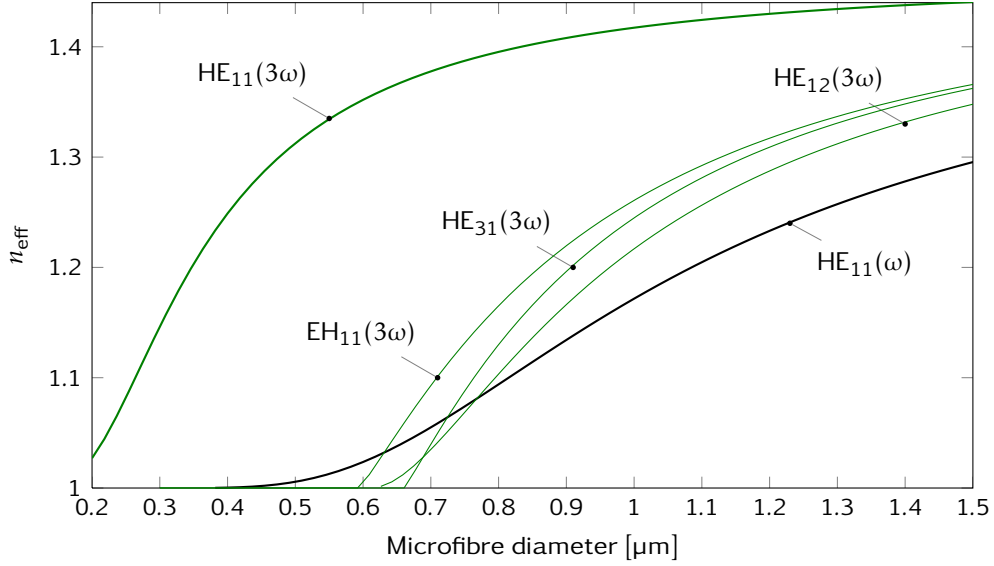


Figure 3: Evolution of the effective indices of the different modes of interest in a silica microfibre according to the microfibre diameter. The wavelengths are 1550 nm (pump, black curve) and 517 nm (third-harmonic, green curves). Phase-matching condition is fulfilled at any intersection of the black curve with one of the green curve.

Since we draw the microfibres manually, the taper waist is not controlled precisely enough to stop the drawing process at a given target diameter. However, provided the waist is smaller than all of the above phase-matching diameters, the phase-matching condition can be met in several localized portions of the transition region of the taper. For each of the three third-harmonic modes considered above, there are two symmetric locations on the microfibre taper where the phase-matching condition is fulfilled, as sketched on Fig.4. This explains why THG is routinely observed in our experiment

without a precise control of the microfibre target diameter. In addition, this also explains the wideband frequency conversion ability of our simple device. Altering the pump wavelength results in a position shift of the phase-matched regions in the taper. Naturally, for a given taper length, the wide bandwidth of the frequency conversion is obtained at the expense of the efficiency of the THG. A large frequency conversion efficiency requires phase matching in the waist itself, preferentially with mode HE_{12} , and this will occur within a narrow bandwidth.

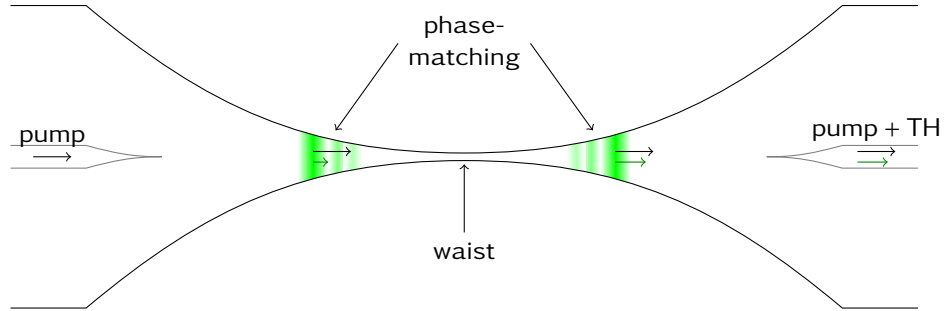


Figure 4: Phase-matched THG occurs in the taper transitions, allowing for broadband conversion

4 THG perspectives with highly nonlinear glasses

Several factors limit the efficiency of THG in silica microfibres, namely the small propagation length over which phase-matching occurs, and the very low nonlinear index of silica. The first point could be solved by developing a complex, automated, accurate drawing method allowing for a long waist with a well-controlled diameter [18]. For the second point, the perspective of using highly-nonlinear glasses for making tapers appears very attractive. Tellurite (TeO_2 based) and chalcogenide (As_2O_3 , for instance) glasses are very good candidates, since their nonlinear indices are more than 20 and 200 times higher than silica, respectively [12, 19]. However, chalcogenide is not well-suited for conversion from 1550 nm to 520 nm, since the transparency range for this glass goes roughly from 600 nm to 10 μm . We will therefore focus on tellurite glasses, with a transmission window in the 0.35-6 μm range.

Calculating the phase-matching diameter for a tellurite microfibre requires a precise knowledge of the indices of the material at pump and third-harmonic wavelengths. For a typical tellurite binary composed of 20 % of NaO_2 and 80 % of TeO_2 , the Sellmeier coefficients given in [20] allow us to calculate the effective indices of the various interesting modes versus the microfibre diameter, as shown on Fig.5. Reducing gradually the microfibre diameter, the first phase-matching condition occurs for the HE_{31} mode at a diameter of 438 nm. However, the corresponding value of the J_3 overlap integral is four times lower than that obtained with the HE_{12} mode. Phase-matching with the latter mode is obtained with an optimum diameter $d_p = 417$ nm. When we look at the effective index, we can see that its value is rather small. Although the index of the bulk

tellurite glass is around 2.0, the effective index is only 1.029, smaller than the effective indices obtained for phase matching within silica microfibres. This last point raises some concern about the actual losses that shall result from the coupling to radiating modes.

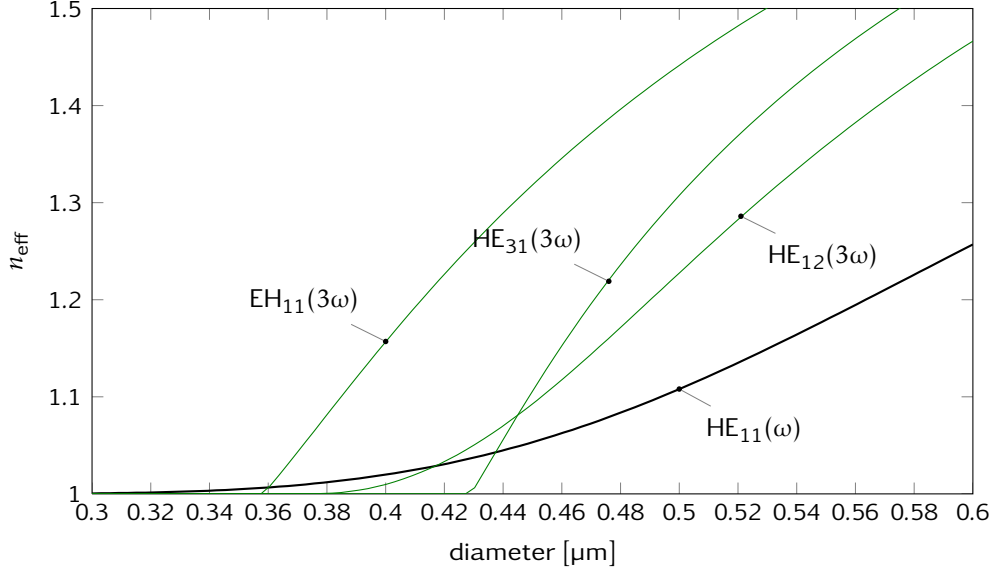


Figure 5: Effective indices of modes in a 20Na₂O tellurite glass at both pump (1560 nm) and TH (520 nm) wavelengths.

Fundamental losses in tapers have been studied by Sumetsky using the theory of nonadiabatic intermode transitions [15]. It is shown that there exists a diameter below which light cannot propagate in the microfibre. This critical diameter depends on the characteristic length of diameter variation, but even for a very smooth taper, it is of the order of $\lambda/10$. By extrapolating Sumetsky's work, which was applied to silica, we are able to evaluate fundamental losses in tellurite and chalcogenide microfibres. If we consider a short taper, whose length is on the order of one centimeter, or below, and if we assume a perfectly processed and homogeneous taper, the intrinsic material loss should be small - typically under 1 dB - at the wavelengths defined here. But it might not be the case for radiative losses. To calculate the latter, we use the same model of taper profile as in Ref. [15]:

$$d(z) = d_{\infty} - \frac{d_{\infty} - d_0}{1 + (z/L)^2}, \quad (4)$$

where $d_{\infty} = 125\mu\text{m}$ is the diameter of the taper far from the center, and d_0 the waist. L is the characteristic length of variation of the diameter. Extrapolating Sumetsky's results with the appropriate refractive indices of tellurite and chalcogenide materials, we obtain the loss curves presented in Fig.6.

First, these results confirm that losses in silica microfibres at THG phase-matching diameter - between 600 and 800 nm - are very low, provided the taper is well drawn all

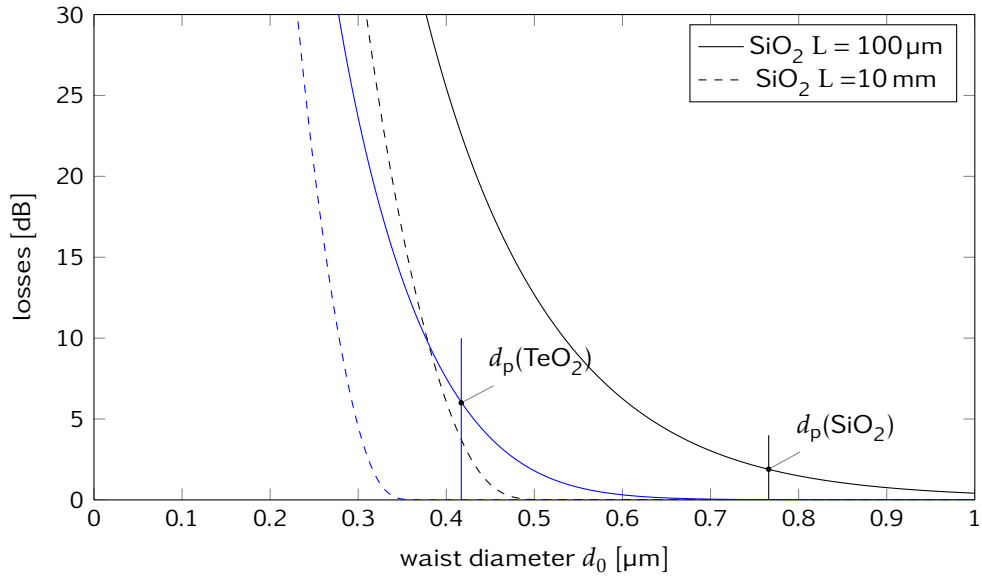


Figure 6: Evaluation of fundamental radiative losses in microfibres at the pump wavelength (1550 nm) using the theory of nonadiabatic intermode transitions. Silica and tellurite microfibres are studied for different characteristic lengths L of diameter variation.

along a length $L \sim 10$ mm. To appreciate the difference for the case of a much shorter taper - it could also be through the influence of microbends in the transition region - we consider another characteristic length: $L = 100 \mu\text{m}$. In the latter case, non negligible losses of 1.9 dB are obtained at the phase-matching diameter.

For tellurite microfibres, in the case of a well drawn taper with ($L = 10$ mm), losses are also negligible. However, they are much more important in the case of a characteristic length of $L = 100 \mu\text{m}$. At the HE_{12} phase-matching diameter, the fundamental pump mode will experience a 6 dB loss while going through the taper. Since THG is a third order process, such loss would result in a threefold attenuation for the third harmonic, i.e. 18 dB less signal.

In order to compare quantitatively the THG efficiencies in silica and tellurite microfibres, we hereafter define an α parameter that takes into account the important quantities discussed above:

$$\alpha = \left(\frac{\omega n_2 |J_3|}{c} \right)^2 l^3, \quad (5)$$

where l represents the radiation induced losses for a $L = 100 \mu\text{m}$ taper, and the unit of α is $\text{m}^{-2}\text{W}^{-2}$. Of course, J_3 and l must be evaluated at the phase-matching diameter for each glass. Each one of these parameters is presented in table 2 as well as the resulting THG efficiency parameter. Our theoretical analysis shows that THG in tellurite glasses could be 100 times more efficient than in silica, even for a steep taper where losses in the transition cannot be ignored. In the case where the loss are negligible for both

Glass	n_2 [m^2W^{-1}]	J_3 [μm^{-2}]	l [dB]	α [$\text{m}^{-2}\text{W}^{-2}$]
Silica	2.7×10^{-20}	1	1.9	3.2×10^{-3}
Tellurite	50×10^{-20}	2.37	6	0.37

Table 2: The different parameters involved in the efficiency of the third-harmonic generation in microfibres of silica or tellurite.

fibres (namely, $L \sim 10\text{mm}$), the efficiency parameters are $1.2 \times 10^{-2} \text{m}^{-2-2}$ for silica and $23 \text{m}^{-2}\text{W}^{-2}$ for tellurite, i.e. approximately 2×10^3 times greater. The perspective of third-harmonic generation in tellurite microfibres is therefore very promising, provided that tapers of good optical quality can be produced, and that efficient coupling with them is achieved.

5 Downconversion and triple photon generation

Triple photon generation (TPG), as the reverse parametric process of THG, is allowed by the same phase-matching conditions. Corona et al. have thus recently suggested that microfibres could be used for TPG [21]. We remind that the extremely small efficiency of spontaneous downconversion has been a recurrent challenging issue for the past decade. Overcoming this issue would open a door to novel experiments and fundamental tests in quantum optics [22]. In this prospect, the wavelengths of choice would be similar as those considered so far in our paper: around 520 nm for the pump, in order to generate photon triplets in the low-loss telecom window of silica, around 1560 nm. We thus suggest that the development of tellurite microfibres, of higher non-linearity than silica, would be beneficial to this quest.

In addition, we can consider another interesting perspective: seeded downconversion for frequency generation in the mid-infrared. As a seed, a broadband supercontinuum extending in the mid-infrared would be used. The pump could be a high-peak-power (kW) pulsed pump at a wavelength of around $1 \mu\text{m}$, or even at around $1.5 \mu\text{m}$. Even with a feeble mid-infrared supercontinuum seed, the conversion efficiency would be incomparably higher than in the spontaneous TPG case. There is one additional difficulty, though: the intense pump should be preferentially coupled to the higher-order mode. Let us consider the case of frequency conversion from 1.55 to $4.65 \mu\text{m}$. Silica cannot be used, since its transparency window stops at around $2.4 \mu\text{m}$. However, either chalcogenide or tellurite glasses are perfectly adapted, from the point of view of transparency and nonlinearity. As before, effective indices for the different modes at play can be calculated to find the phase-matching diameter, and the loss can be evaluated for a taper of given characteristic length by the theory of nonadiabatic intermode transitions.

The results are compiled in Fig.7: phase-matching diameters are found at $1.36 \mu\text{m}$ in tellurite fibres and 980 nm for chalcogenide. Losses could again be a problem in the case of a short characteristic length, particularly for chalcogenide glasses, with a 13 dB attenuation for a $L = 100 \mu\text{m}$. However, from the drawing point of view, the diameters

at play are relatively large, which would help in obtaining characteristic lengths larger than 1 mm. The realization of smooth, well-controlled tapers of several centimeter long made of highly nonlinear glasses is definitely the largest current technological challenge. Once overcome, no doubt the above applications will soar.

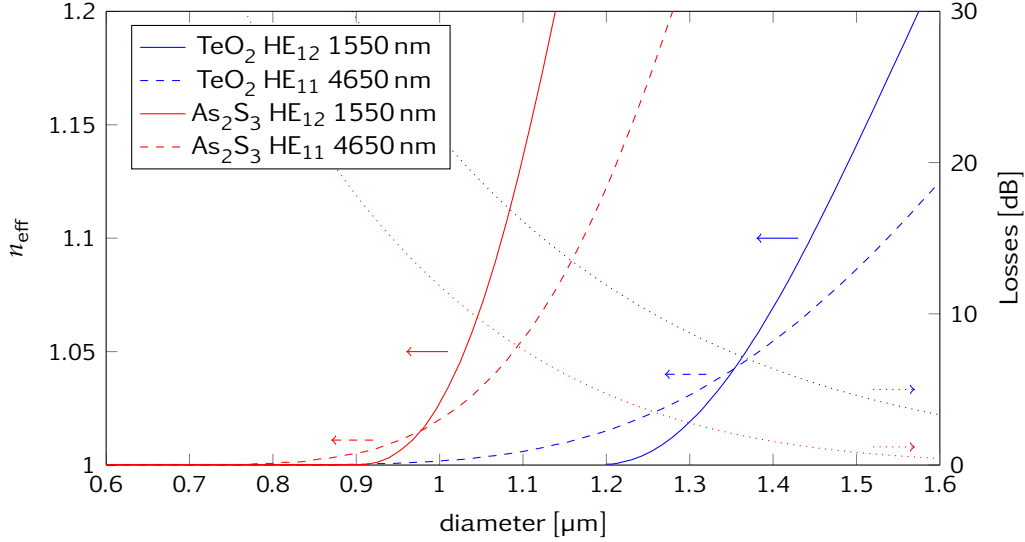


Figure 7: Index variation of the HE_{11} (4650 nm) and HE_{12} (1550 nm) modes in tellurite and chalcogenide as a function of the diameter of the microfiber. Phase-matching diameters for triple photon generation are $1.36 \mu\text{m}$ in tellurite fibers and 980 nm in chalcogenide fibers. Losses, calculated for a characteristic taper transition length $L=100 \mu\text{m}$, are represented with dotted lines and on the right y -axis.

6 Conclusions

In this paper, third-harmonic generation in manually-drawn silica taper is demonstrated and interpreted. In particular, it is shown that phase-matching occurs between the fundamental pump mode and three higher-order modes of the third-harmonic for a given diameter at each side of the microfiber's waist. To improve the conversion efficiency, we discussed the opportunity of using highly nonlinear glasses, and studied the case of tellurite glass microfibers. Despite the increased losses - due to nonadiabatic intermode transitions- the expected efficiency remain several orders of magnitude larger in tellurite microfibers than in silica microfibers. The key issue is now at the technological level, where improvements of the homogeneity and of the overall quality of the microfibers drawn out of tellurite compounds are awaited. Finally, we provide an outlook concerning parametric down-conversion in the mid-infrared, by examining the phase matching conditions for triple photon generation at around 4650 nm in tellurite or chalcogenide glasses. As in the case of THG, phase-matching is found possible for a

given diameter, and losses can be kept below reasonably low values.

References

- [1] X. Jiang, Q. Yang, G. Vienne, Y. Li, L. Tong, J. Zhang, and L. Hu, "Demonstration of microfiber knot laser," *Appl. Phys. Lett.* **89**, 143513 (2006).
- [2] F. Xu, P. Horak, and G. Brambilla, "Optical microfiber coil resonator refractometric sensor," *Opt. Express* **15**, 7888–7892 (2007).
- [3] G. Vienne, P. Grelu, X. Pan, Y. Li, and L. Tong, "Theoretical study of microfiber resonator devices exploiting a phase shift," *J. Opt. A: Pure Appl. Opt.* **10**, 025303 (2008).
- [4] F. Le Kien, V. I. Balykin, and K. Hakuta, "Atom trap and waveguide using a two-color evanescent light field around a subwavelength-diameter optical fiber," *Phys. Rev. A* **70**, 063403 (2004).
- [5] A. Coillet, B. Cluzel, G. Vienne, P. Grelu, and F. de Fornel, "Near-field characterization of glass microfibers on a low-index substrate," *Applied Physics B: Lasers and Optics* **101**, 291–295 (2010).
- [6] R. R. Gattass, G. T. Svacha, L. Tong, and E. Mazur, "Supercontinuum generation in submicrometer diameter silica fibers," *Opt. Express* **14**, 9408–9414 (2006).
- [7] D.-I. Yeom, E. C. Mägi, M. R. E. Lamont, M. A. F. Roelens, L. Fu, and B. J. Eggleton, "Low-threshold supercontinuum generation in highly nonlinear chalcogenide nanowires," *Opt. Lett.* **33**, 660–662 (2008).
- [8] V. Grubsky and J. Feinberg, "Phase-matched third-harmonic uv generation using low-order modes in a glass micro-fiber," *Optics Communications* **274**, 447–450 (2007).
- [9] A. Coillet, G. Vienne, and P. Grelu, "Potentialities of glass air-clad micro- and nanofibers for nonlinear optics," *J. Opt. Soc. Am. B* **27**, 394–401 (2010).
- [10] U. Wiedemann, K. Karapetyan, C. Dan, D. Pritzkau, W. Alt, S. Irsen, and D. Meschede, "Measurement of submicrometre diameters of tapered optical fibres using harmonic generation," *Opt. Express* **18**, 7693–7704 (2010).
- [11] T. Lee, Y. Jung, C. A. Codemard, M. Ding, N. G. R. Broderick, and G. Brambilla, "Broadband third harmonic generation in tapered silica fibres," *Opt. Express* **20**, 8503–8511 (2012).
- [12] A. Lin, A. Rysanyanskiy, and J. Toulouse, "Tunable third-harmonic generation in a solid-core tellurite glass fiber," *Opt. Lett.* **36**, 3437–3439 (2011).

- [13] K. Bencheikh, S. Richard, G. Mélin, G. Krabshuis, F. Gooijer, and J. A. Levenson, "Phase-matched third-harmonic generation in highly germanium-doped fiber," *Opt. Lett.* **37**, 289–291 (2012).
- [14] E. C. Mägi, L. B. Fu, H. C. Nguyen, M. R. Lamont, D. I. Yeom, and B. J. Eggleton, "Enhanced kerr nonlinearity in sub-wavelength diameter As_2Se_3 chalcogenide fiber tapers," *Opt. Express* **15**, 10324–10329 (2007).
- [15] M. Sumetsky, "How thin can a microfiber be and still guide light?" *Opt. Lett.* **31**, 870–872 (2006).
- [16] L. Tong, R. R. Gattass, J. B. Ashcom, S. He, J. Lou, M. Shen, I. Maxwell, and E. Mazur, "Subwavelength-diameter silica wires for low-loss optical wave guiding," *Nature* **426**, 816–819 (2003).
- [17] V. Grubsky and A. Savchenko, "Glass micro-fibers for efficient third harmonic generation," *Opt. Express* **13**, 6798–6804 (2005).
- [18] S. Pricking and H. Giessen, "Tapering fibers with complex shape," *Opt. Express* **18**, 3426–3437 (2010).
- [19] J. H. V. Price, T. M. Monro, H. Ebendorff-Heidepriem, F. Poletti, P. Horak, V. Finazzi, J. Y. Y. Leong, P. Petropoulos, J. C. Flanagan, G. Brambilla, M. Feng, and D. J. Richardson, "Mid-IR supercontinuum generation from nonsilica microstructured optical fibers," *Journal of selected topics in quantum electronics* **13**, 738–749 (2007).
- [20] G. Ghosh, "Sellmeier coefficients and chromatic dispersions for some tellurite glasses," *Journal of the American Ceramic Society* **78**, 2828–2830 (1995).
- [21] M. Corona, K. Garay-Palmett, and A. U'Ren, "Experimental proposal for the generation of entangled photon triplets by third-order spontaneous parametric down conversion in optical fibers," *Opt. L* **36**, 190–192 (2011).
- [22] S. Richard, K. Bencheikh, B. Boulanger, and J. A. Levenson, "Semiclassical model of triple photons generation in optical fibers," *Opt. Lett.* **36**, 3000–3002 (2011).